Research Square

Preprints are preliminary reports that have not undergone peer review.
They should not be considered conclusive, used to inform clinical practice,
or referenced by the media as validated information.

Macular Neovascularization Subtype Determines Visual Consequences of Early Fibro-atrophic Remodelling in Neovascular AMD: PRECISE Study Report 11

Dun Jack Fu

d.fu@nhs.net

NIHR Biomedical Research Centre, Moorfields Eye Hospital NHS Foundation Trust and UCL Institute of Ophthalmology, London, UK https://orcid.org/0000-0003-2852-6912

Livia Faes

Cantonal Hospital Winterthur https://orcid.org/0000-0002-4159-3960

Heena Syed Kubravi

Kimberly Spooner

https://orcid.org/0000-0001-5096-3786

Sobha Sivaprasad

Moorfields Eye Hospital

Article

Keywords:

Posted Date: February 3rd, 2026

DOI: https://doi.org/10.21203/rs.3.rs-8575526/v1

License: This work is licensed under a Creative Commons Attribution 4.0 International License.
Read Full License

Additional Declarations: There is no conflict of interest

Version of Record: A version of this preprint was published at Eye on September 17th, 2026. See the published version at https://doi.org/10.1038/s41433-026-04858-7.

Abstract

Purpose: To investigate how baseline optical coherence tomography (OCT) biomarkers of early fibro-atrophic remodeling defined as well-delineated hyperreflective material [wdHRM] associated with atrophic surrogates and fluid resolution influence early visual outcomes in treatment-naïve neovascular age-related macular degeneration (nAMD), and whether effects differ by macular neovascularization (MNV) subtype.

Methods: In the PRECISE cohort completing aflibercept 2 mg induction of three loading injections, baseline wdHRM and fluid status at Visit 4 (V4 mean = 112 days) were examined as independent predictors of best-corrected visual acuity (BCVA). Regression models included MNV subtype, baseline BCVA and V4 fluid status.

Results: Baseline wdHRM independently predicted poorer short-term vision. Paradoxically, the BCVA penalty attributable to wdHRM was greater in eyes achieving complete fluid resolution (6.4 letters worse) than in those with residual fluid (3.4 letters worse), revealing that fluid itself masks the true structural deficit. The impact of wdHRM varied by MNV subtype: Type 3 MNV showed the largest visual penalty (9 letters), moderate penalties in Types 1, 2 and mixed (4 letters), and negligible effects in polypoidal choroidal vasculopathy. Baseline wdHRM is strongly associated with outer retinal disruption and choroidal hypertransmission, particularly in Type 3 MNV, suggesting a fibro-atrophic rather than purely fibrotic state.

Conclusions: The impact of OCT biomarkers indicative of fibrosis is heterogeneous across MNV subtypes and modified by fluid resolution. wdHRM, particularly in Type 3 MNV, likely represents mixed fibro-atrophic remodeling, explaining disproportionate early visual penalties despite low overall fibrosis incidence. These findings refine baseline prognostication and emphasize the need to counsel patients based on these likely consequences of MNV subtype.

Introduction

Fibrosis is one of the most formidable barriers to sustained visual recovery in exudative neovascular age-related macular degeneration (nAMD), even in the era of anti-angiogenic therapy. [1] Despite major therapeutic advances, fibrotic sequelae remain common, developing in up to one fifth of treated eyes by one year, approximately one third by two years, and in the majority by five years. [1] Importantly, about 60% of the 5-year fibrotic burden accumulates within the first treatment year. [1–8] In real-world cohorts, macular fibrosis is consistently associated with substantially worse visual function at presentation and persistently poorer outcomes during follow-up, in a severity-dependent manner. [1,5,9] In those studies, patients with subretinal scarring were more likely to experience clinically meaningful visual acuity decline than eyes without fibrosis. [1,10]

On histopathology, fibrosis in nAMD denotes excessive extracellular-matrix deposition, predominantly collagen, fibronectin and laminin, by myofibroblast-rich fibrovascular tissue within the subretinal or sub-RPE compartment. [11,12] Although *in vivo* imaging is used to infer fibrosis, definitive identification remains challenging because operational criteria vary and tissue confirmation is impractical in clinical care. [12] Contemporary practice prioritises spectral-domain optical coherence tomography (OCT), where fibrosis has been operationalised as sub-RPE or subretinal hyperreflective material ([S]HRM) that has evolved to a homogeneous, plaque with well-delineated anterior borders (wdHRM). Yet (S)HRM and wdHRM are not synonymous with fibrosis. They are descriptive OCT terms encompassing exudative subretinal hyperreflective exudation (SHE), haemorrhage and non-exudative components (e.g. fibrovascular tissue), and remain inconsistently used across studies. [12,13] The temporal behaviour of these lesions under treatment is not fully characterized. After anti-angiogenic therapy induction, the exudative fraction of HRM can dissipate, while any fibrotic scaffold persists or contracts. [14,15] Baseline or cross-sectional OCT alone can therefore not reliably label all hyperreflective material as persistent “fibrosis” as a portion is treatment-reversible exudation. Accordingly, several groups distinguish (S)HRM with a fuzzy, temporally dynamic and structurally ill-defined subretinal component (e.g. exudative component) from wdHRM, with the latter consistently associated with poorer visual outcomes unless boundary remodelling has occurred. [16–19]

Increasing clinicoradiologic evidence indicates that fibrosis and macular atrophy are not mutually exclusive endpoints in treated nAMD but often co-localize, with thin residual subretinal HRM detectable within areas labelled as atrophy. This fibro-atrophic continuum is sometimes termed atrosis which may confer risks distinct from primary (non-neovascular) geographic atrophy. [20]

The heterogeneity in fibrosis propensity, atrophy and visual prognosis across MNV subtypes introduces further complexity. Observational and trial analyses converge on higher fibrosis risk in Type 2- or mixed lesions, lower rates in Type 3 MNV, and intermediate risk (and often sub-RPE in phenotype) in Type 1 MNV (including polypoidal choroidal vasculopathy [PCV]).[1,21,22] These subtype patterns imply that unstratified associations may be misleading and must be analyzed with subtype-specific context.

Several clinically relevant uncertainties persist during the induction phase of treatment for neovascular AMD. The prevalence and interplay of structural biomarkers indicative of both fibrotic and atrophic remodelling at presentation remain incompletely characterized. Furthermore, the early trajectory of fibrosis-associated OCT features under therapy has not been systematically quantified, and their independent prognostic value for short-term visual outcomes is not fully delineated. It also remains unclear whether adverse visual associations are attenuated in eyes that achieve complete anatomical resolution of IRF and SRF, or whether such effects differ across MNV subtypes.

To this end, we analysed PRECISE, which is a large, contemporary, multicentre programme assessing patients with nAMD receiving aflibercept (*2mg/0.05ml, Bayer*). PRECISE has defined short-term anatomic and functional endpoints after three monthly injections (post-induction- or “loading” phase, Visit 4 [V4]), quantified early residual fluid (ERF) such as sub- (SRF) or intraretinal fluid (IRF) and its determinants, and

identified baseline OCT features, associated with worse presenting vision and suboptimal best-corrected visual acuity (BCVA) after completion of therapy induction. [23–29] In the present analysis cohort, wdHRM was present in 14.6% before starting anti-angiogenic therapy. [28,29] At presentation in nAMD, the evolution under therapy, and short-term prognostic impact of fibrosis- and atrophy-related OCT biomarkers are still poorly defined, including whether their adverse visual effects vary by MNV subtype.

METHODS

Study Design and Ethical Considerations

This was a multicentre observational analysis within the PRECISE programme of treatment-naïve nAMD eyes initiated on aflibercept 2 mg and assessed at baseline and after completion of three-monthly injections (post-"loading" or therapy induction, V4). The dataset taken forward for analysis comprised 2036 eyes with tracked baseline and V4 OCT and BCVA measurements drawn from the consolidated PRECISE data freeze used for this report. Patient recruitment occurred between December 2019 and August 2021 across United Kingdom centres with harmonised protocols. Aflibercept treatment schedules and visit timing that frame the present analysis have been published elsewhere. All procedures adhered to the Declaration of Helsinki with local institutional approvals and consent according to PRECISE governance as described in previous publications.[23–29]

Imaging Acquisition and Central Reading

Participating sites acquired spectral-domain OCT (*Spectralis; Heidelberg Engineering*) with a standardised 6 × 6 mm fovea-centred macular cube and foveal B-scans. A central reading workflow harmonised feature definitions across sites as per PRECISE reports. Graders were masked to outcomes where applicable. Baseline imaging underwent double grading to enhance reliability, whereas V4 imaging was only subject to single grading due to study logistics and resource constraints.

Neovascular subtype (Type 1-, Type 2/mixed-, Type 3 MNV, and polypoidal choroidal vasculopathy [PCV]) was determined from structural OCT morphology. PCV was recorded where clinically diagnosed at the treating site. No systematic invasive angiography was undertaken.

Our dataset does not encode topographic co-localisation between wdHRM, and ellipsoid zone- (EZ), external limiting membrane (ELM)- loss or hypertransmission (HTM), so we refrain from inferring the "atrosis" phenomenon spatially.

Pre-specified Operational Definitions

(S)HRM: hyperreflective material with a dynamic and ill-defined subretinal component (e.g. exudative component)

wdHRM: Homogeneous hyperreflectivity and sharply delineated anterior margins with or without boundary remodelling consistent with fibro-cellular tissue ("fibrosis"), as adjudicated by PRECISE image

graders at baseline. Ascertainment was OCT-only (no mandatory colour fundus photography or angiography).

Outcomes, Covariates and Effect Modifiers

The primary outcome was BCVA, measured in ETDRS letters, at V4. Secondary outcomes included the prevalence of fibrosis and macular atrophy biomarkers at V4, as well as analyses of BCVA stratified by fibrosis biomarker status in conjunction with retinal “dryness” and by neovascular subtype. These contrasts aimed to elucidate the differential impact of fibrotic evolution and disease phenotype on visual outcomes following therapy.

Prespecified covariates for outcome adjustment included baseline BCVA, age, sex, ethnicity, MNV subtype, and the absence of IRF and SRF at V4.

Statistical Analysis

Analyses were conducted on the per-eye dataset with only one eye considered per patient. We used multivariable linear regression for V4 BCVA, estimating adjusted mean differences (β) with robust (sandwich) standard errors, clustered by patient. Covariates were entered as described above. Interaction terms included fibrosis × ”dryness” (absence of SRF and IRF) and fibrosis × MNV subtype. Where interactions were statistically significant, we computed estimated marginal means (EMMs) and simple contrasts to quantify the fibrosis-related BCVA penalty within dryness strata and within each subtype.

Sensitivity analyses assessed robustness to additional adjustment for atrophy (baseline and/or Visit 4), restriction to anatomically “dry” eyes at V4, an alternative dryness definition limited to the central subfield, exclusion of PCV and accounting for centre effects via a random intercept or generalized estimating equations framework.

Eyes missing V4 pathology variables were excluded from models requiring those variables.

RESULTS

Study Cohort Demographics and Clinical Characteristics

We analysed 2036 treatment-naïve eyes with exudative nAMD that completed the three-dose induction with a median time from first injection to V4 of about 112 days. Mean baseline age was 79.4 years (standard deviation [SD] 7.8), including 60.8% females in the cohort. 95.3% of patients were of Caucasian ethnicity. Mean BCVA improved 4.6 letters from baseline (mean 58.0 letters, SD 14.5) to V4 (mean 62.6 letters, SD 15.2). SRF (83%) and IRF (50.8%) at baseline were reduced to 37.6% and 21.7% at V4 respectively. At V4, 49.7% of eyes showed complete resolution of IRF and SRF. (*Tables 1 and 2*).

Evolution of Fibrosis Biomarkers across Therapy Induction

At baseline, (S)HRM was present in 58.3% of eyes overall, distributed as foveal and extrafoveal (43.2%), foveal-only (4.2%), and extra-foveal-only (11.0%). Mean (S)HRM width was 885 μm (SD 1010) and mean height 99.9 μm (SD 138). By Visit 4 (V4), wdHRM prevalence increased from 14.5% to 21.1%.

Following anti-angiogenic therapy induction (loading phase), 7.3% of eyes had persistent wdHRM, 7.1% showed resolution of baseline wdHRM, 13.7% developed new wdHRM by V4 despite being wdHRM-free at baseline (incident wdHRM), and 71.7% remained free of wdHRM at both baseline and V4 (*data not shown*). Eyes that went on to develop wdHRM by V4 already carried a higher HRM burden at baseline, with more frequent presence of (S)HRM, greater horizontal extent and greater height ($p \leq 0.001$). (*Table 2*)

Co-occurrence of Fibrosis and Macular Atrophy Biomarkers

At baseline, HTM was present in 21.1% (430/2036) of eyes. EZ and ELM were frequently ungradable at presentation (EZ ungradable 41.7%; ELM ungradable 42.3%), reflecting lesion burden and scan limitations. Fovea-involving EZ- and ELM-loss at baseline were roughly twice as frequent in eyes with fibrosis biomarkers at V4 than without. HTM at V4 was detected in 95.6% of eyes with fibrotic biomarkers versus 68.8% of eyes lacking these imaging signs ($p < 0.001$), whereas baseline HTM prevalence was similar between the two groups.(*Table 2*) Conversely, among eyes with gradable HTM, those with HTM at V4 had lower BCVA at both baseline (56 vs 62 letters) and V4 (60 vs 68 letters, $p < 0.001$) than eyes without HTM. Baseline HTM was more frequent in eyes that showed HTM at V4 (26.2% vs 6.8%, $p < 0.001$), and these eyes showed substantially higher rates of fovea-involving EZ- and ELM-loss at baseline. Baseline wdHRM was also more common in eyes that showed HTM at V4 (18.2% vs 3.7%, $p < 0.001$), and wdHRM at V4 observed in 27.1% of eyes with HTM compared with 3.7% of eyes without HTM ($p < 0.001$). Because spatial co-localization was not available, these findings should be interpreted as eye-level associations rather than lesion-level confirmation that wdHRM directly overlies areas of HTM or EZ/ELM loss (i.e., “atrophy”).(*Table 3*)

Interaction Between Baseline Fibrosis Biomarkers and Fluid Resolution

To quantify the joint associations of baseline wdHRM and fluid resolution on visual outcome, we fitted a multivariable linear regression model for BCVA at V4 that included baseline wdHRM, as well as presence of SRF and IRF at V4, their interaction, adjusted for baseline BCVA, age, sex, ethnicity and MNV subtype. Baseline wdHRM and presence of fluid at V4 were both independently associated with poorer BCVA ($p < 0.001$). The interaction term between baseline wdHRM and presence of fluid at V4 was statistically significant ($p = 0.029$), indicating that the fibrosis-associated visual penalty differed by fluid status. Among eyes that did not have SRF or IRF at V4, baseline wdHRM was associated with an estimated 6.4-letter reduction in adjusted mean BCVA compared with eyes without baseline wdHRM (56.0 vs 62.4

letters), whereas in eyes that had fluid the corresponding penalty was 3.4 letters (56.9 vs 60.3 letters) (Fig. 1).

Visual Outcomes Stratified by MNV Subtype

Neovascular subtype distributions at baseline were: Type 1 MNV (39.2%), Type 2- and mixed MNV (32.8%), Type 3 MNV (21.7%), and PCV (6.3%) (*Table 4*). Baseline wdHRM was most frequent in Type 2- or mixed MNV (23.1%) and PCV (14.8%), and less common in Type 3- (12.2%) and Type 1 MNV (8.9%). By V4, wdHRM remained most frequent in Type 2- and mixed MNV (27.4%) and PCV (30.5%), compared with Type 3- (19.5%) and Type 1 MNV (15.0%). Type 3 MNV had the highest prevalence of HTM at baseline (38.9%), followed by PCV (20.3%), Type 1 (18.4%) and Type 2- and mixed MNV (12.7%). Baseline SRF was almost universal in PCV (99.2%) and common in Type 1- (93.1%) and Type 2- and mixed MNV (91.9%), but less frequent in Type 3 MNV (46.6%). By V4, complete fluid resolution was most often achieved in Type 3 MNV (66.1%) and least in PCV (37.5%).

In extended multivariable models including an interaction between baseline wdHRM and MNV subtype, the visual penalty associated with baseline wdHRM differed significantly across subtypes (global interaction $p = 0.016$). After adjustment for baseline BCVA, age, sex, ethnicity and absence of IRF and SRF at V4, baseline wdHRM in Type 3 MNV conferred an almost 9-letter deficit at V4 (53.8 vs 62.5 letters). The corresponding deficits were 4.3 letters in Type 2 (57.9 vs 62.2) and 3.7 letters in Type 1 (58.2 vs 61.9). In PCV, the short-term visual impact of baseline wdHRM was negligible (58.2 vs 58.3 letters).

DISCUSSION

In a large, treatment-naïve nAMD cohort completing induction therapy with aflibercept, baseline biomarkers of fibrosis and persistent retinal fluid after completion of therapy induction were each independently associated with poorer short-term BCVA. The visual penalty attributable to the occurrence of fibrosis biomarkers at baseline was not static. Rather, it varied depending on whether exudative fluid was resolved completely by V4 and on the underlying MNV subtype.

The fibrosis biomarker-associated visual deficit paradoxically increased in eyes that achieved complete fluid resolution (6.4 letters worse) compared to eyes with persistent fluid (3.4 letters worse). This counterintuitive finding reveals the mechanism underlying visual loss in different contexts. When exudation persists, visual acuity depression reflects the combined contribution of active disease and structural pathology. In anatomically “dry” eyes, the full deficit attributable to fibrosis biomarkers becomes apparent because fluid effects have been removed. This observation suggests that baseline fibrosis biomarkers may establish a functional ceiling on achievable visual outcomes that persists despite optimal anatomical fluid control. Thus clinicians should not assume complete visual recovery in “dry” eyes when baseline fibrosis biomarkers are present.

Fibro-Atrophic Remodelling Rather Than Pure Fibrosis

The strong association between fibrosis and atrophy biomarkers supports that wdHRM frequently indexes broader tissue remodelling affecting multiple retinal layers rather than a single histologic entity confined to the subretinal space. HTM was detected in almost all eyes with wdHRM at V4 (versus 80.6 percent without). This strong co-occurrence, despite similar baseline HTM prevalence between groups, indicates that evolution from baseline fibrosis biomarkers to V4 outcomes involves not merely scar accumulation but active tissue remodelling encompassing both fibrotic and atrophic processes.[30,31] Recent molecular and histopathologic studies indicate that atrophy and fibrosis in nAMD are mechanistically linked and not merely competing or sequential endpoints. Both processes are driven, in part, by epithelial–mesenchymal transformation (EMT) of RPE cells. EMT contributes to subretinal fibrosis by enabling RPE cells to acquire migratory and contractile myofibroblastic properties, depositing extracellular matrix and collagen in the subretinal space. Simultaneously, EMT-mediated RPE dedifferentiation can impair cell survival and function, accelerating the development of atrophy through loss of metabolic and trophic support for the photoreceptors. Thus, the coexistence of atrophy (particularly in areas of HTM) and fibrosis biomarkers may reflect a shared biology of chronic injury and maladaptive wound repair rather than strictly separate pathways. [32]

Recent literature proposes the term "atrosis" to denote atrophy with (S)HRM on OCT, recognizing that atrophy and fibrosis are not mutually exclusive endpoints in treated nAMD but rather often co-localize.[20]

Neovascular Subtype-specific Visual Impact

The effect of baseline fibrosis biomarkers differed substantially across MNV subtypes. Type 3 MNV showed the most severe visual penalty (approximately 9 letters worse), followed by moderate penalties in Type 2 and mixed lesions (4.3 letters) and Type 1 MNV (3.8 letters), with negligible effects in PCV. This pattern appears counterintuitive given that Type 2 and mixed lesions carry the highest cumulative fibrosis incidence at 1 to 3 years.[21] Yet the dissociation between fibrosis incidence and early visual burden across subtypes is not paradoxical when one considers the underlying tissue biology. Type 3 MNV, originating in the inner retinal layers and progressing toward the RPE over time, may create a distinct pathophysiological landscape from subretinal Type 2 disease. [33,34] The PRECISE data revealed that Type 3 eyes comprise the highest proportion of baseline IRF and achieve the highest rates of complete fluid resolution. Notably, Type 3 lesions also show the highest baseline prevalence of macular atrophy biomarkers and the strongest association between presence of fibrosis biomarkers at baseline and outer retinal structural disruption, with EZ- and ELM-loss occurring approximately twice as frequently in eyes developing fibrosis biomarkers. This constellation suggests that in Type 3 MNV, presence of baseline fibrosis biomarkers frequently marks a mixed fibro-atrophic state involving glial activation, intraretinal remodelling, and photoreceptor loss rather than pure subretinal fibrosis.[33] The disproportionate visual penalty despite lower overall fibrosis incidence may reflect that tissue loss has already occurred within the retina itself, rendering it mechanistically irreversible despite successful fluid

control. The known heterogeneity in cellular responses across MNV subtypes provides mechanistic underpinning for these observations. Myofibroblasts can arise from RPE EMT transition, perivascular fibroblasts, and macrophage-to-myofibroblast transition. Different subtypes may preferentially activate distinct cellular sources. Type 2 lesions may feature predominantly RPE-derived myofibroblasts producing organized subretinal plaque-like material, while Type 3 lesions may involve greater contributions from intraretinal glial responses and localized photoreceptor loss, resulting in qualitatively different tissue phenotypes.[11,14,18,35–37] Anti-angiogenic therapy effectively compresses the exudative fraction, and while scarring accrues when RPE integrity is breached, much of the baseline wdHRM burden may initially reflect treatment-responsive exudation rather than fixed fibrotic substrate. The slower initial visual penalty in Type 2 and mixed lesions thus reflects the opportunity for partial improvement as fluid resolves.[12,14,21,38]

In PCV without significant subretinal haemorrhage or RPE tears, fibrovascular tissue may predominantly be found underneath the RPE rather than in the subretinal space. Sub-RPE or extrafoveal fibrotic tissue may spare the photoreceptor layer and can therefore be compatible with preserved vision. This anatomic compartmentalization may explain why presence of fibrosis biomarkers at baseline confers negligible short-term visual penalty in PCV despite substantial structural involvement.

Limitations

Several important limitations merit emphasis.

First, although baseline grading followed strict procedures, V4 regrading was performed without formal dual-grading. This asymmetry is expected to increase measurement error at V4 and, if misclassification is nondifferential, would bias associations toward the null, making effect sizes more likely to be underestimated than inflated.

Second, PRECISE does not encode precise topographic co-localization between fibrosis and atrophy biomarkers as only eye-level co-occurrence is available. Therefore, the atrosis hypothesis that fibrosis and atrophy biomarkers share the same anatomic locus cannot be definitively tested.

Finally, MNV subtype classification relied on structural OCT morphology without mandatory multimodal imaging at every visit, potentially biasing subtype-stratified analyses.

Implications for Research and Practice

Spatial registration techniques for multimodal imaging modalities, including OCT and fundus autofluorescence, may permit precise mapping of the relationships between fibrosis and atrophy biomarkers, thereby refining phenotype characterization. Crucially, prospective histopathologic studies, including tissue sampling in well-phenotyped patients are needed to anchor imaging-defined lesions in definitive tissue composition and cellular context.

For clinical practice, the neovascular subtype context proves essential for interpreting fibrosis biomarkers. In PCV, sub-RPE fibrovascular tissue carries less immediate visual consequence than subretinal scar in Type 2 MNV, whereas Type 2- and mixed lesions may demonstrate a rapid fibrosis trajectory that warrants close structural surveillance even when visual acuity initially improves. In Type 3 MNV, the presence of baseline fibrosis biomarkers signals a mixed fibro-atrophic state with substantial visual consequences. The large visual penalty and high baseline atrophy prevalence argue for realistic expectations about functional recovery and careful consideration of whether additional therapies targeting atrophy might prove beneficial.

Conclusion

PRECISE refines the short-term visual meaning of early fibrosis biomarkers in treatment-naïve exudative nAMD. The resolution of exudative fluid after induction paradoxically amplifies the apparent penalty of fibrosis biomarkers by removing confounding fluid effects, and the underlying MNV subtype similarly modifies the visual impact, with the largest penalty observed in Type 3 MNV, moderate effects in Types 1, 2 and mixed, and negligible effects in PCV. Fibrosis biomarkers show strong associations with OCT biomarkers of atrophy, suggesting it represents a fibro-atrophic state rather than a single pathologic substrate, and its visual import varies fundamentally across neovascular subtypes. The PRECISE data invite prospective, multimodal, imaging-guided studies of subtype-aware therapeutic strategies designed to clarify tissue composition across subtypes and enable mechanistically informed treatment selection.

References

1. Cheong KX, Cheung CMG, Teo KYC. Review of fibrosis in neovascular age-related macular degeneration. Am. J. Ophthalmol. 2023; 246: 192–222.
2. Chakravarthy U, Harding SP, Rogers CA, Downes S, Lotery AJ, Dakin HA, et al. A randomised controlled trial to assess the clinical effectiveness and cost-effectiveness of alternative treatments to Inhibit VEGF in Age-related choroidal Neovascularisation (IVAN). Health Technol. Assess. 2015; 19(78): 1–298.
3. Daniel E, Pan W, Ying G-S, Kim BJ, Grunwald JE, Ferris FL 3rd, et al. Development and course of scars in the Comparison of Age-related Macular Degeneration Treatments Trials. Ophthalmology. 2018; 125(7): 1037–1046.
4. Daniel E, Ying G-S, Kim BJ, Toth CA, Ferris F 3rd, Martin DF, et al. Five-year follow-up of nonfibrotic scars in the Comparison of Age-Related Macular Degeneration Treatments Trials. Ophthalmology. 2019; 126(5): 743–751.
5. Teo KYC, Joe AW, Nguyen V, Invernizzi A, Arnold JJ, Barthelmes D, et al. Prevalence and risk factors for the development of physician-graded subretinal fibrosis in eyes treated for neovascular age-related macular degeneration. Retina. 2020; 40(12): 2285–2295.
6. Gillies M, Arnold J, Bhandari S, Essex RW, Young S, Squirrell D, et al. Ten-year treatment outcomes of neovascular age-related macular degeneration from two regions. Am. J. Ophthalmol. 2020; 210:

116–124.

7. Finger RP, Puth M-T, Schmid M, Barthelmes D, Guymer RH, Gillies M. Lifetime outcomes of anti-vascular endothelial growth factor treatment for neovascular age-related macular degeneration. JAMA Ophthalmol. 2020; 138(12): 1234–1240.
8. Romano F, Cozzi E, Airaldi M, Nassisi M, Viola F, Aretti A, et al. Ten-year incidence of fibrosis and risk factors for its development in neovascular age-related macular degeneration. Am. J. Ophthalmol. 2023; 252: 170–181.
9. Casalino G, Stevenson MR, Bandello F, Chakravarthy U. Tomographic biomarkers predicting progression to fibrosis in treated neovascular age-related macular degeneration: A multimodal imaging study. Ophthalmol. Retina. 2018; 2(5): 451–461.
10. Nguyen CL, Gillies MC, Nguyen V, Daien V, Cohn A, Banerjee G, et al. Characterization of poor visual outcomes of neovascular age-related macular degeneration treated with anti-vascular endothelial growth factor agents. Ophthalmology. 2019; 126(5): 735–742.
11. Tenbrock L, Wolf J, Boneva S, Schlecht A, Agostini H, Wieghofer P, et al. Subretinal fibrosis in neovascular age-related macular degeneration: current concepts, therapeutic avenues, and future perspectives. Cell Tissue Res. 2022; 387(3): 361–375.
12. Bachmeier I, Armendariz BG, Yu S, Jäger RJ, Ebneter A, Glittenberg C, et al. Fibrosis in neovascular age-related macular degeneration: A review of definitions based on clinical imaging. Surv. Ophthalmol. 2023; 68(5): 835–848.
13. Shah VP, Shah SA, Mrejen S, Freund KB. Subretinal hyperreflective exudation associated with neovascular age-related macular degeneration. Retina. 2014; 34(7): 1281–1288.
14. Armendariz BG, Chakravarthy U. Fibrosis in age-related neovascular macular degeneration in the anti-VEGF era. EYE. 2024; 38(17): 3243–3251.
15. Pauleikhoff D, Yu S, Bachmeier I, Armendariz BG, Bormann E, Pauleikhoff L. Hyperreflective material evolution patterns during long term anti-VEGF therapy in neovascular age-related macular degeneration. Arbeitsphysiologie. 2025; 263(4): 957–964.
16. Willoughby AS, Ying G-S, Toth CA, Maguire MG, Burns RE, Grunwald JE, et al. Subretinal hyperreflective material in the Comparison of age-Related Macular Degeneration Treatments Trials. Ophthalmology. 2015; 122(9): 1846–53.e5.
17. Roberts PK, Zotter S, Montuoro A, Pircher M, Baumann B, Ritter M, et al. Identification and quantification of the angiofibrotic switch in neovascular AMD. Invest. Ophthalmol. Vis. Sci. 2019; 60(1): 304–311.
18. Roberts PK, Schranz M, Motschi A, Desissaire S, Hacker V, Pircher M, et al. Morphologic and microvascular differences between macular neovascularization with and without subretinal fibrosis. Transl. Vis. Sci. Technol. 2021; 10(14): 1.
19. Yu S, Bachmeier I, Hernandez-Sanchez J, Garcia Armendariz B, Ebneter A, Pauleikhoff D, et al. Hyperreflective material boundary remodeling in neovascular age-related macular degeneration: A post hoc analysis of the AVENUE trial. Ophthalmol. Retina. 2023; 7(11): 990–998.

20. Lindenberg S, Nittala MG, Verma A, Fitzgerald MEC, Velaga SB, Bhisitkul RB, et al. Subretinal hyperreflective material in regions of atrophy and fibrosis in eyes with neovascular age-related macular degeneration. Can. J. Ophthalmol. 2025; 60(1): 26–34.
21. Lenhof S, Kodjikian L, Gascon P, Gadiollet E, Feldman A, De Bats F, et al. Subretinal fibrosis occurrence according to macular neovascularisation subtypes in neovascular age-related macular degeneration. Acta Ophthalmol. 2025; 103(2): e104–e117.
22. Cheung CMG, Grewal DS, Teo KYC, Gan A, Mohla A, Chakravarthy U, et al. The evolution of fibrosis and atrophy and their relationship with visual outcomes in Asian persons with neovascular age-related macular degeneration. Ophthalmol. Retina. 2019; 3(12): 1045–1055.
23. Chandak S, Gurudas S, Pakeer Muhammed R, Keskin A, Thottarath S, Ghanchi F, et al. Visual outcome following initiation of first injection versus after three monthly doses of aflibercept 2 mg for treatment naïve age-related macular degeneration to inform clinical trial designs: PRECISE Report No. 6. Eye. 2025; 39(11): 2194–2203.
24. Montesel A, Pakeer Muhammed R, Chandak S, Kazantzis D, Thottarath S, Chandra S, et al. Subretinal transient hyporeflectivity in neovascular age-related macular degeneration and its response to a loading phase of aflibercept: PRECISE report 4. EYE. 2024; 38(13): 2596–2602.
25. Thottarath S, Gurudas S, Chandak S, Patel PJ, Kotagiri A, Pearce I, et al. Impact of treat and extend criteria on proportions that can be extended after loading phase of 2 mg aflibercept therapy for neovascular age related macular degeneration: PRECISE Report 5. EYE. 2024; 38(14): 2737–2743.
26. Sivaprasad S, Chandak S, Gurudas S, Muhammed RP, Kazantzis D, Ghanchi F, et al. Factors associated with achieving various visual acuity outcomes during loading doses of aflibercept 2mg for treatment naïve exudative age-related macular degeneration: PRECISE Study Report 7. Research Square. 2024. Available at: http://dx.doi.org/10.21203/rs.3.rs-5416918/v1 [Accessed October 28, 2025].
27. Chorev M, Haderlein J, Chandra S, Menon G, Burton BJL, Pearce I, et al. A multi-modal AI-driven cohort selection tool to predict suboptimal non-responders to aflibercept loading-phase for neovascular age-related macular degeneration: PRECISE study report 1. J. Clin. Med. 2023; 12(8): 3013.
28. Chandra S, Gurudas S, Burton BJL, Menon G, Pearce I, Mckibbin M, et al. Associations of presenting visual acuity with morphological changes on OCT in neovascular age-related macular degeneration: PRECISE Study Report 2. EYE. 2024; 38(4): 757–765.
29. Chandra S, Gurudas S, Pearce I, Mckibbin M, Kotagiri A, Menon G, et al. Baseline characteristics of eyes with early residual fluid post loading phase of aflibercept therapy in neovascular AMD: PRECISE study report 3. EYE. 2024; 38(7): 1301–1307.
30. Teo KYC, Zhao J, Ibrahim FI, Fenner B, Chakravarthy U, Cheung CMG. Features associated with vision in eyes with subfoveal fibrosis from neovascular age-related macular degeneration. Am. J. Ophthalmol. 2024; 261: 121–131.

31. Kim JH, Chang YS, Kim JW, Kim CG, Lee DW, Kim YJ. Morphologic features associated with fibrotic scarring after anti–vascular endothelial growth factor therapy in polypoidal choroidal vasculopathy. Retina. 2018; 38(11): 2168–2176.
32. Higashijima F, Hasegawa M, Yoshimoto T, Kobayashi Y, Wakuta M, Kimura K. Molecular mechanisms of TGFβ-mediated EMT of retinal pigment epithelium in subretinal fibrosis of age-related macular degeneration. Front. Ophthalmol. (Lausanne). 2022; 2: 1060087.
33. Faes L, Bijon J, Bacci T, Freund KB. Review of type 3 macular neovascularization in age-related macular degeneration: no DRAMA (Deep Retinal Age-related Microvascular Anomalies). EYE. 2024. Available at: https://pubmed.ncbi.nlm.nih.gov/39394372/ [Accessed December 16, 2024].
34. Spaide RF, Jaffe GJ, Sarraf D, Freund KB, Sadda SR, Staurenghi G, et al. Consensus Nomenclature for Reporting Neovascular Age-Related Macular Degeneration Data: Consensus on Neovascular Age-Related Macular Degeneration Nomenclature Study Group. Ophthalmology. 2020; 127(5): 616–636.
35. Ishikawa K, Kannan R, Hinton DR. Molecular mechanisms of subretinal fibrosis in age-related macular degeneration. Exp. Eye Res. 2016; 142: 19–25.
36. Little K, Ma JH, Yang N, Chen M, Xu H. Myofibroblasts in macular fibrosis secondary to neovascular age-related macular degeneration - the potential sources and molecular cues for their recruitment and activation. EBioMedicine. 2018; 38: 283–291.
37. Luo X, Yang S, Liang J, Zhai Y, Shen M, Sun J, et al. Choroidal pericytes promote subretinal fibrosis after experimental photocoagulation. Dis. Model. Mech. 2018; 11(4). Available at: http://dx.doi.org/10.1242/dmm.032060 [Accessed November 19, 2025].
38. Han HY, Park SM, Lee JH, Kim CG, Kim JW, Cho HJ, et al. Outcomes and predictive factors for fluid resolution following three loading injections of faricimab for treatment-naïve neovascular age-related macular degeneration. Sci. Rep. 2025; 15(1): 938.

Tables

Tables are available in the Supplementary Files section.

Figures

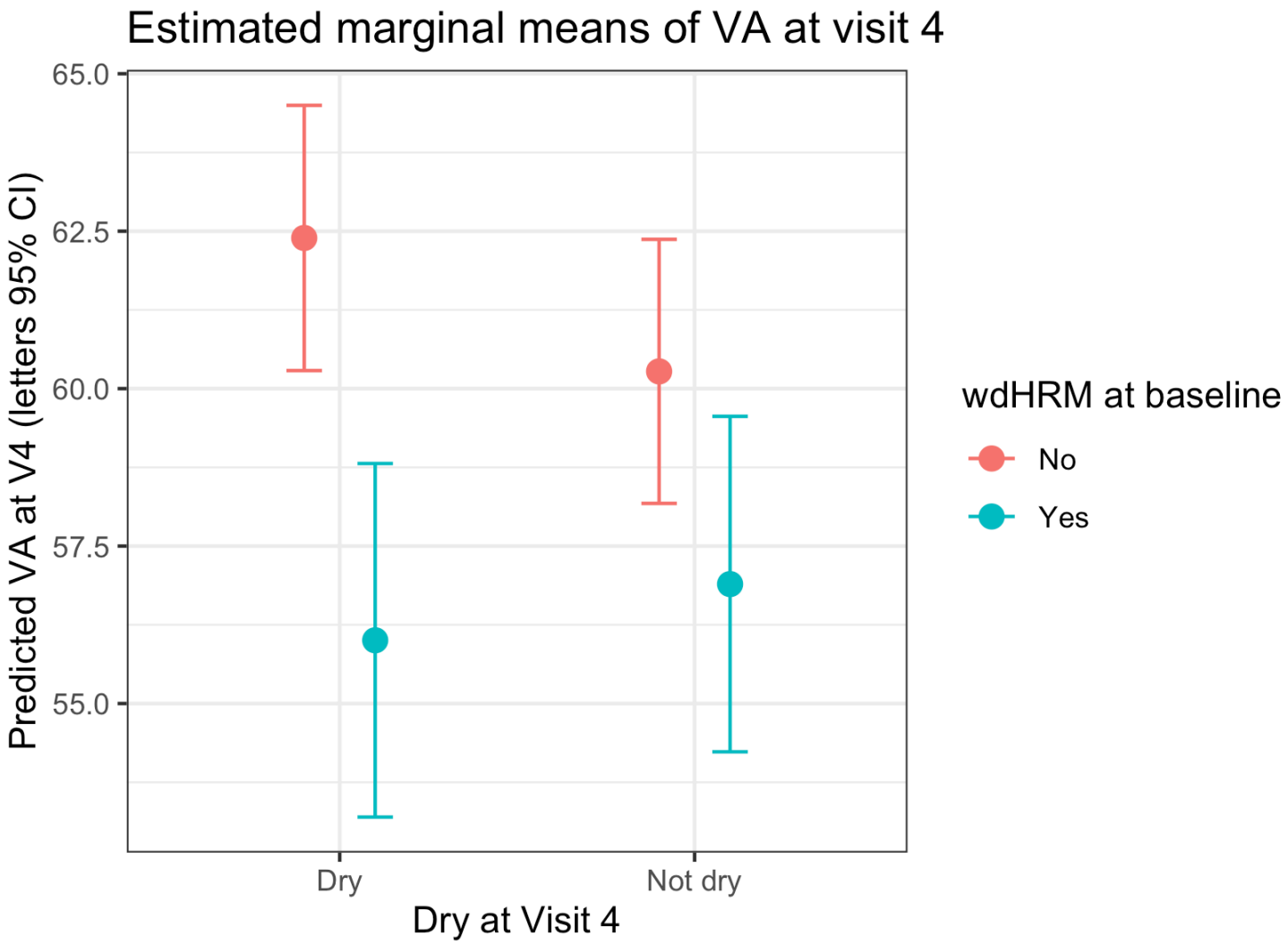


Figure 1

Interaction Between Baseline wdHRM and Fluid Resolution on Adjusted BCVA at Visit 4. Estimated marginal means (EMMs) of BCVA at Visit 4 (V4) (ETDRS letters) with 95% confidence intervals, stratified by V4 dryness (Dry: absence of both IRF and SRF at V4; Not dry: residual IRF and/or SRF at V4) and baseline wdHRM (Yes/No). EMMs were derived from a multivariable linear regression model including baseline wdHRM, V4 fluid status, and their interaction, adjusted for baseline BCVA, age, sex, ethnicity, and MNV subtype. The figure illustrates that the wdHRM-associated visual deficit is larger among eyes achieving complete fluid resolution than among eyes with residual fluid. Abbreviations: BCVA, best-corrected visual acuity; CI, confidence interval; EMM, estimated marginal mean; ETDRS, Early Treatment Diabetic Retinopathy Study; IRF, intraretinal fluid; SRF, subretinal fluid; V4, Visit 4; wdHRM, well-delineated hyperreflective material; MNV, macular neovascularization.

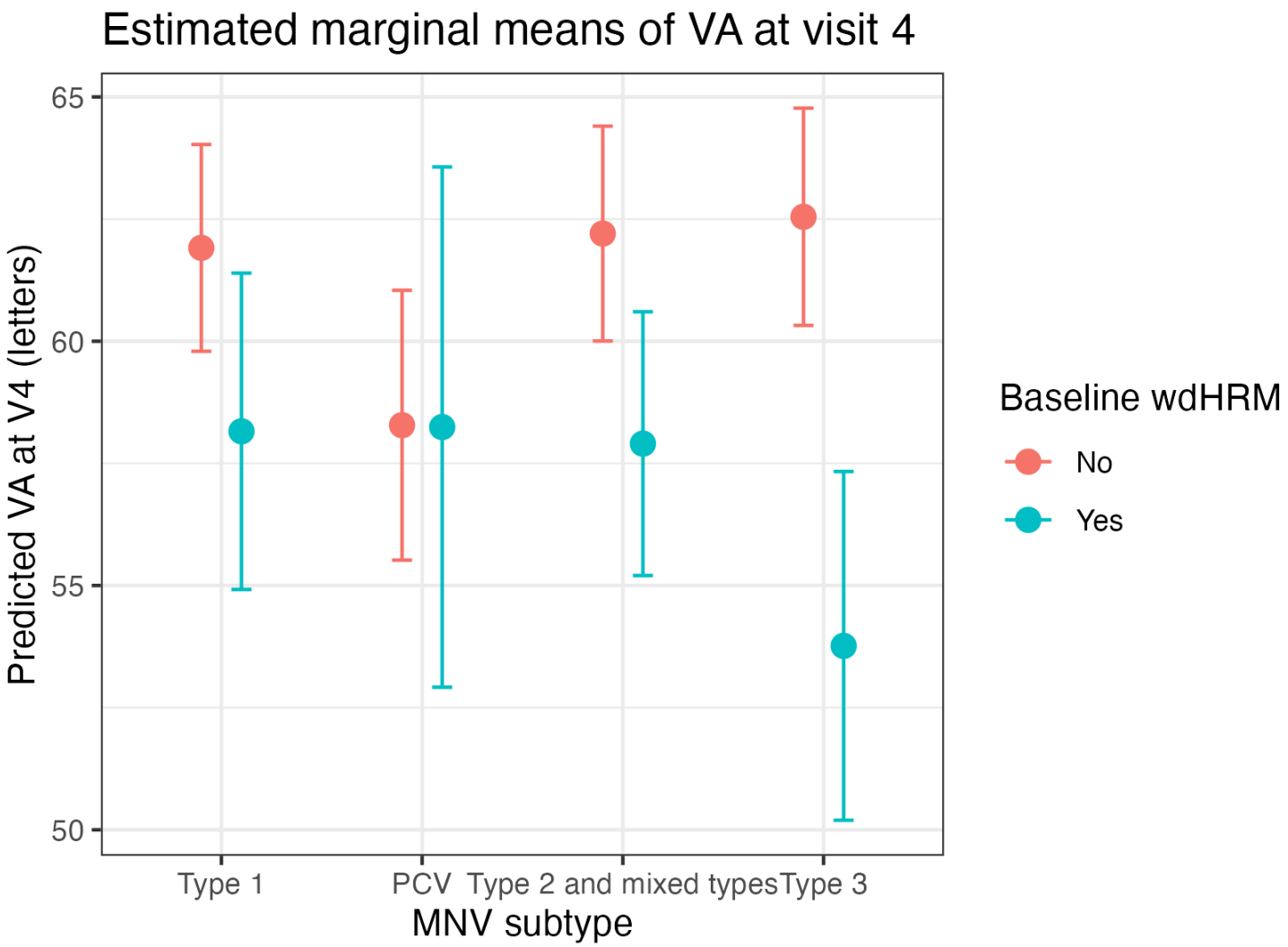


Figure 2

Adjusted BCVA at Visit 4 by MNV Subtype and Baseline wdHRM Status.

Estimated marginal means (EMMs) of BCVA at V4 (ETDRS letters) with 95% confidence intervals across MNV subtypes (Type 1, PCV, Type 2/mixed, Type 3), stratified by baseline wdHRM (Yes/No). EMMs were obtained from a multivariable linear regression model including an interaction between baseline wdHRM and MNV subtype, adjusted for baseline BCVA, age, sex, ethnicity, and V4 fluid status (absence of IRF and SRF). The figure demonstrates heterogeneity in the wdHRM-associated visual penalty across subtypes, with the largest deficit observed in Type 3 MNV. Abbreviations: BCVA, best-corrected visual acuity; CI, confidence interval; EMM, estimated marginal mean; ETDRS, Early Treatment Diabetic Retinopathy Study; IRF, intraretinal fluid; SRF, subretinal fluid; MNV, macular neovascularization; PCV, polypoidal choroidal vasculopathy; V4, Visit 4; wdHRM, well-delineated hyperreflective material.

Supplementary Files

This is a list of supplementary files associated with this preprint. Click to download.

- TABLELEGENDS.docx
- Table.1.docx
- Table.2.docx
- Table.3.docx
- Table.4.docx